JOURNAL OF SOLID STATE CHEMISTRY **134,** 1–4 (1997)
ARTICLE NO. SC977505

Neutron Diffraction Study of $LiNi_{0.8}Mn_{0.2}O_2$

A. Hirano, R. Kanno,[1] and Y. Kawamoto

Department of Chemistry, Faculty of Science, Kobe University, Nada, Kobe, Hyogo 657, Japan

Y. Nitta and K. Okamura

Technology Laboratory, Matsushita Battery Industrial Co., Ltd. 1, Matsushita-cho, Moriguchi, Osaka 570, Japan

T. Kamiyama

Institute of Materials Science, University of Tsukuba, Tsukuba, Ibaraki 305, Japan

and

F. Izumi

National Institute for Research in Inorganic Materials, Tsukuba, Ibaraki 305, Japan

Received February 27, 1997; accepted June 2, 1997

Structure of the layered oxide, $LiNi_{0.8}Mn_{0.2}O_2$, was determined by TOF neutron powder diffraction using space group $R\bar{3}m$. Its ionic distribution was determined to be $[Li_{0.956}Ni_{0.044}]_{3a}$–$(Ni_{0.791}Mn_{0.209})_{3b}O_2$. Slightly higher temperature of the synthesis caused the disordered arrangement of the Ni ions in the Li 3*a* sites. Nevertheless, the manganese ions introduced into the lattice were situated only at the Ni sites. The structural changes caused by the manganese substitution are clarified, and the relationship between the ionic distribution and the cathodic properties of the lithium cells is discussed. © 1997 Academic Press

1. INTRODUCTION

Transition metal oxides $LiMO_2$($M = 3d$ transition metal) with layered rocksalt structures have been studied for possible use as insertion electrodes in 4 V rechargeable lithium batteries (1–4). In this structure, Li and M atoms composing alternate layers occupy the octahedral sites of a cubic close packed (ccp) oxygen array making up a rhombohedral structure. Among these oxides, the lithium nickel oxide, $LiNiO_2$, is currently a promising cathode candidate for its lower cost and higher energy density than the lithium cobalt cathodes. However, its nonstoichiometry significantly degrades charge and discharge characteristics (5), and nearly stoichiometric $LiNiO_2$ is rather difficult to obtain because of the high vapor pressure of lithium at the calcination temperature (6).

[1] To whom correspondence should be addressed.

In order to improve the cycling capacity, solid solutions such as $LiNi_{1-x}Mn_xO_2$ (7–9), $LiNi_{1-x}Co_xO_2$ (10, 11), $LiNi_{1-x}Fe_xO_2$ (12) have been studied; among these solid solutions, the $LiNi_{1-x}Mn_xO_2$ system showed excellent cycling characteristics and is a promising cathode candidate for practical lithium cells (8, 9). Lithium manganese oxides have several compositions, such as $LiMn_2O_4$, $LiMnO_2$, and Li_2MnO_3. $LiMn_2O_4$ has a spinel structure, $LiMnO_2$ has an orthorhombic corrugated layer structure, which consists of a ccp oxygen array and cation sheets made up of an alternating pair of Li and Mn rows, and Li_2MnO_3 has the layered rock salt structure with cationic (111) planes alternatively occupied by Li and ($LiMn_2$) layers. The solid solutions based on $LiNiO_2$ and the lithium manganese oxides might therefore be formed along the tie lines, $LiNiO_2$–$LiMnO_2$ or $LiNiO_2$–Li_2MnO_3. Previously, the solid solutions in these systems were prepared and disributions of Li, Ni, and Mn in them were discussed in the X-ray difraction study (7). A slightly disordered arrangement at both the Li and Ni sites in the $R\bar{3}m$ structure has been proposed, and the existence of Mn^{4+} ions was indicated.

Since the cationic distribution in the host affects the charge–discharge characteristics, it is important to elucidate its cationic distribution. Neutron diffraction is expected to be a powerful means to clarify structural details, because of the difference in the coherent scattering lengths of Li, Mn, and Ni atoms ($b_c(\mathrm{Li}) = -0.1900 \times 10^{-12}$ cm, $b_c(\mathrm{Mn}) = -0.3730 \times 10^{-12}$ cm, $b_c(\mathrm{Ni}) = 1.034 \times 10^{-12}$ cm, $b_c(\mathrm{O}) = 0.5803 \times 10^{-12}$ cm). In the present study, we determined the structure of $LiNi_{0.8}Mn_{0.2}O_2$ by means of neutron powder

0022-4596/97 $25.00
Copyright © 1997 by Academic Press
All rights of reproduction in any form reserved.

diffraction. Further, we discuss the relationship between the cycling characteristics of the lithium cells using $LiNi_{0.8}Mn_{0.2}O_2$ cathodes, and their cationic distribution is also discussed.

2. EXPERIMENTAL

The solid solution, $LiNi_{0.8}Mn_{0.2}O_2$, was prepared by heating appropriate molar ratios of LiOH, $MnCO_3$ and $Ni(OH)_2$ (LiOH, High Purity Chemicals Laboratory Co., Ltd., >99.9% purity; $MnCO_3$, High Purity Chemicals Latoratory Co., Ltd., >99.9% purity; $Ni(OH)_2$, High Purity Chemicals Laboratory Co., Ltd., >99.9% purity). They were mixed, pelletized, and then heated at 850 °C in an oxygen atmosphere. The composition of the sample was determined by inductive coupled plasma spectroscopy (ICP) for the Ni and Mn contents, and by atomic abosrption spectroscopy for the Li content. The molar ratio of metals was Li:Ni:Mn = 1.00:0.80:0.20, resulting in the formula $Li_{1.00}Ni_{0.80}Mn_{0.20}O_2$.

Neutron diffraction data for $LiNi_{0.8}Mn_{0.2}O_2$ were taken at 295 K on a time-of-flight (TOF) neutron powder diffractometer, VEGA, at the KENS pulsed spallation neutron source at the National Laboratory for High Energy Physics (KEK). The specimen of (ca. 10 g) was contained in a cylindrical vanadium cell of dimensions 5 mm in radius, 55 mm in height, and 200 μm in thickness. The structural parameters were refined with RIETAN (13).

3. RESULTS AND DISCUSSION

Intensity data for interplanar spacings between 0.5 and 2.6 Å were used for Rietveld analysis. We refined the structure parameters of $LiNi_{0.8}Mn_{0.2}O_2$ with space group $R\bar{3}m$ using the following structural model: Li at 3*a* (0, 0, 0), Ni at 3*b* (0, 0, 1/2), O at 6*c* (0, 0, *z*) with $z \approx 0.25$. During the refinement, the total amounts of lithium, nickel, and manganese were fixed at the values determined by the ICP and atomic absorption spectroscopy.

The strucutral parameters were refined using structural models with three different cationic distributions as follows: (i) Li and Mn ions situated in the Li 3*a* site and Ni ions in the Ni 3*b* site, (ii) Li and Ni ions situated in the Li 3*a* site and Ni and Mn ions in the Ni 3*b* site, (iii) Mn ions distributed in both the Li 3*a* and Ni 3*b* sites. The occupation parameters both for the Li 3*a* and Ni 3*b* sites were refined using the constraints that the total occupancy at each site is unity and that the Ni/Mn ratio is 0.8/0.2. The structural model (i), however, led to a negative *g* value for the Mn ions at the Li 3*a* site. Furthermore, no significant amount of Mn ions was detected in the Li 3*a* site using the model (iii) ($g \approx 0.004$). These results clearly indicate that the Mn ions are situated only in the Ni 3*b* site, and the slight disordered arrangement in the Li 3*a* sites is caused only by the Ni ions. Finally, anisotropic thermal parameters were assigned for the Li 3*a*, Ni 3*b*, and O 6*c* sites. Table 1 lists final *R* factors and lattice and structural parameters with their estimated standard deviations in parentheses. Figure 1 illustrates the profile fit and difference pattern for $LiNi_{0.8}Mn_{0.2}O_2$; the calculated pattern fits the observed one fairly well. Table 2 gives interatomic distances and bond angles calculated with ORFFE (14), together with the distances between two subsequent oxygen layers, O–Li–O and O–Ni–O. Corresponding data for $Li_{1.01}NiO_2$ systhesized at 700°C (6) are also indicated.

The cationic distribution in the sample was determined to be $[Li_{0.956}Ni_{0.044}]_{3a}(Ni_{0.791}Mn_{0.209})_{3b}O_2$. The slightly disordered arrangement of Ni ions at the Li 3*a* site was caused

TABLE 1
Rietveld Refinement Results for $LiNi_{0.8}Mn_{0.2}O_2$

Atom	Site	*g*	*x*	*y*	*z*	*B* (Å^2)
Li(1)	3*a*	0.9495(17)[a]	0	0	0	1.57[b]
Ni(1)	3*a*	0.0505	0	0	0	= *B*(Li(1))
Ni(2)	3*b*	0.7899	0	0	1/2	0.45[b]
Mn	3*b*	0.2101	0	0	1/2	= *B*(Ni(1))
O	6*c*	1	0	0	0.24173(6)	0.90[b]

Atom	U_{11} (Å^2)[c]	U_{22} (Å^2)	U_{33} (Å^2)	U_{12} (Å^2)	U_{13} (Å^2)	U_{23} (Å^2)
Li(1)	0.0188(16)	$=U_{11}$	0.015(3)	$=U_{22}/2$	0	0
Ni(2)	0.054(2)	$=U_{11}$	0.0045(3)	$=U_{22}/2$	0	0
O	0.0120(9)	$=U_{11}$	0.0061(19)	$=U_{22}/2$	0	0

Note. $a = 2.87974(10)$ Å, $c = 14.2273(3)$ Å, $R_{wp} = 4.46$, $R_p = 3.45$, $S = R_{wp}/R_e = 1.18$, $R_I = 2.89$, $R_F = 1.83$.

[a] Numbers in parentheses are estimated standard deviations of the last significant digit. Occupancies without deviations were fixed under the constraint that the total occupancies of 3*a* and 3*b* sites are unity.

[b] Equivalent isotropic thermal parameter, B_{eq}.

[c] The form of the anisotropic temperature factor is $\exp[-2\pi^2(h^2a^{*2}U_{11} + k^2b^{*}U_{22} + l^2c^{*2}U_{33} + 2hka^*b^*U_{11} + 2hla^*c^*U_{13} + 2klb^*c^*U_{23})]$.

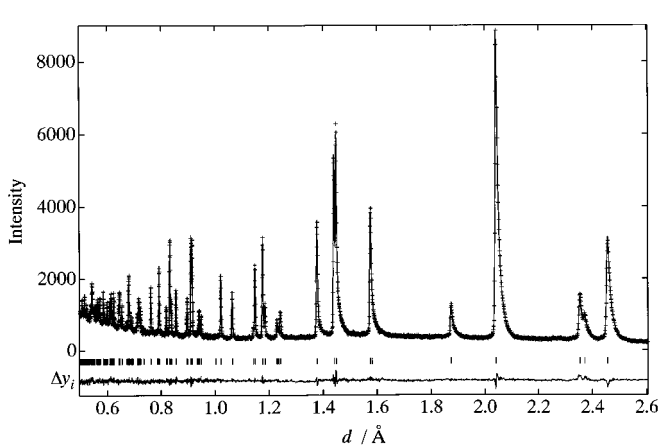

FIG. 1. Observed, calculated, and difference plots of $LiNi_{0.8}Mn_{0.2}O_2$. The solid lines are calculated intensities, plus (+) overlying them are observed intensities, and Δy_i is the difference between observed and calculated intensities.

TABLE 2
Interatomic Distances (Å), Bond Angles (°), and Interlayer Distances (Å)

	$LiNi_{0.8}Mn_{0.2}O_2$	$Li_{1.00}Ni_{1.01}O_2$ (6)
Interatomic distances		
Li(1)–O^{i}	2.1125(5) × 6	2.1154(14) × 6
Ni(2)–O^{ii}	1.9761(4) × 6	1.9692(12) × 6
Bond angles		
O^{iii}–Li(1)–O^{iv}	85.93(2) × 6	83.24(15) × 6
O^{v}–Ni(2)–O^{vi}	93.54(2) × 6	94.77(19) × 6
Interlayer distances		
O–Li(1)–O	2.450	2.450
O–Ni(2)–O	2.292	2.282

Note. Symmetry codes: (i) $\frac{2}{3}-x, \frac{1}{3}-y, \frac{1}{3}-z$; (ii) $\frac{2}{3}+x, \frac{1}{3}+y, \frac{1}{3}+z$; (iii) $-\frac{1}{3}-x, \frac{1}{3}-y, \frac{1}{3}-z$; (iv) $-\frac{1}{3}-x, -\frac{2}{3}-y, \frac{1}{3}-z$; (v) $-\frac{1}{3}+x, \frac{1}{3}+y, \frac{1}{3}+z$; (vi) $-\frac{1}{3}+x, -\frac{2}{3}+y, \frac{1}{3}+z$.

by the higher synthesis temperature of 850°C. The relationship between the synthesis temperatures and the nonstoichiometry was previously determined for $Li_{1-x}Ni_{1+x}O_2$ (6, 15), and the higher synthesis temperature 850°C led the disordered cationic arrangements of Ni ions in the Li site ($x \approx 0.05$). The occupancy of Ni ions in the Li site ($g \approx 0.044$) in $LiNi_{0.8}Mn_{0.2}O_2$ is consistent with that observed for $Li_{1-x}Ni_{1+x}O_2$ synthesized at 850°C. Nevertheless, manganese ions were found only in the Ni 3*b* sites with no significant occupancies at the lithium 3*a* sites, which indicates the preference of the Mn ions for the Ni 3*b* sites.

Figure 2 shows an ORTEP drawing of $LiNi_{0.8}Mn_{0.2}O_2$. The thermal parameters determined for the $LiNi_{0.8}Mn_{0.2}O_2$ system are comparable to those determined for $Li_{1.01}NiO_2$ (6). The thermal parameters at the Li 3*a* and Ni 3*b* sites are almost isotropic, while those in the O 6*c* site is slightly anisotropic along the *c* plane.

The changes in interatomic distance with the introduction of Mn ions in $LiNiO_2$ are summarized as follows. No significant differences were observed between $LiNi_{0.8}Mn_{0.2}O_2$ and $Li_{1.01}Ni_{1.00}O_2$ for the Li–O and the O–Li–O distances. On the other hand, the Ni–O (1.9761(4) Å) and O–Ni–O (2.292 Å) distances in $LiNi_{0.8}Mn_{0.2}O_2$ are slightly larger than those in $Li_{1.01}NiO_2$ (Ni–O, 1.9692(12) Å; O–Ni–O, 2.282 Å), which is explained by the introduction of larger Mn^{3+} ions in the Ni site. All the structural changes indicated are consistent with the idea that the Mn ions occupy only Ni 3*b* site. The average oxidation state of the metal ions is 2.92+, and the $M^{2+}:M^{3+}$ ratio is 0.08:0.92 if we assume the mixed valence state. The oxidation state of the manganese ions is not, however, confirmed in the present sutdy.

Our crystal data clarified the slightly disordered arrangement of Ni ions in the Li 3*a* site for the sample synthesized at 850°C. In $Li_{1-x}Ni_{1+x}O_2$, the disordered arrangement of $x \approx 0.05$ significantly degraded its charge–discharge characteristics of the lithium cells. The charge–discharge characteristics of the cell consisting of the $LiNi_{0.8}Mn_{0.2}O_2$ sample used for our neutron diffraction experiment showed a low cycling capacity, which was caused by the disordered Ni ions in the Li 3*a* site. However, the lithium cells composed of the $LiNi_{0.8}Mn_{0.2}O_2$ cathode synthesized at 700°C in an oxygen atmosphere showed higher cycling capacities of ca. 185 mA h/g without a significant degradation. The improvement was obviously caused by the order, arrangement in the Li site. The cycling characteristics are also dependent on the stability of deintercalated structures, $Li_{1-y}Ni_{0.8}Mn_{0.2}O_2$. Further structural studies on deinercalated phases are necessary to elucidate the degradation of the cycling characteristics.

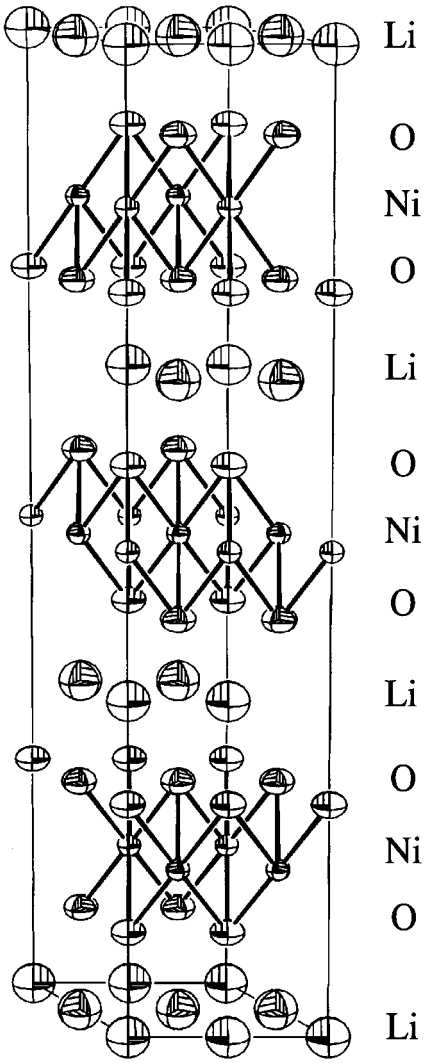

FIG. 2. The ORTEP drawing of the structure for $LiNi_{0.8}Mn_{0.2}O_2$.

ACKNOWLEDGMENTS

R.K. thanks the Kansai Research Foundation for Technology Promotion for financial assistance. This work was supported partly by a Grant-in-Aid for Scientific Research on Priority Areas (No. 260), a Grant-in-Aid for Developmental Scientific Research (No. 06555262) from The Ministry of Education, Science and Culture, and a NEDO Interational Joint Research Grant.

REFERENCES

1. K. Mizushima, P. C. Jones, P. J. Wiseman, and J. B. Goodenough, *Mater. Res. Bull.* **15,** 783 (1980).
2. M. G. S. R. Thomas, W. I. F. David, J. B. Goodenough, and P. Groves, *Mater. Res. Bull.* **20,** 1137 (1985).
3. J. R. Dahn, U. von Sacken, and C. A. Michal, *Solid State Ionics* **44,** 87 (1990).
4. J. R. Dahn, U. van Sacken, M. W. Juzkow, and H. Al-Janaby, *J. Electrochem. Soc.* **138,** 2207 (1991).
5. H. Arai, S. Okada, H. Ohtsuka, and M. Ichimura, *in* "Proceedings of the Symposium on New Sealed Rechargeable Batteries and Supercapacitors," p. 451. The Electrochemical Society Inc., Pennington, NJ, 1993.
6. R. Kanno, H. Kubo, Y. Kawamoto, T. Kamiyama, F. Izumi, Y. Takeda, and M. Takano, *J. Solid State Chem.* **110,** 216 (1994).
7. E. Rossen, C. D. W. Jones, and J. R. Dahn, *Solid State Ionics* **57,** 311 (1992).
8. Y. Nitta, K. Okamura, K. Haraguchi, S. Kobayashi, and A. Ohta, *in* "Proceedings of the 34th Battery Symposium in Japan," p. 45. Battery Division, The Electrochemical Soc. Japan, Hiroshima, Japan, 1993.
9. Y. Nitta, K. Okamura, K. Haraguchi, S. Kobayashi, and A. Ohta, *J. Power Source* **54,** 511 (1995).
10. C. Delmas and I. Saadoune, *Solid State Ionics* **53–56**, 370 (1992).
11. T. Ohzuku, H. Komori, K. Sawai, and T. Hirai, *Chem. Express* **5,** 733 (1990).
12. J. N. Reimers, E. Rossen, C. D. Jones, and J. R. Dahn, *Solid State Ionics* **61,** 335 (1993).
13. F. Izumi, "The Rietveld Method" (R. A. Young, Ed.), Chap. 13. Oxford Univ. Press, Oxford, 1993.
14. W. R. Busing, K. O. Martin, and H. A. Levy, Oak Ridge National Laboratory. Report ORNL-TM-306 (1964).
15. A. Hirano, R. Kanno, Y. Kawamoto, Y. Takeda, K. Yamaura, M. Takano, K. Ohyama, M. Ohashi, and Y. Yamaguchi, *Solid State Ionics* **78,** 123 (1995).